HHS Public Access

Author manuscript

J Immunol. Author manuscript; available in PMC 2016 October 15.

Published in final edited form as:

J Immunol. 2015 October 15; 195(8): 3654–3664. doi:10.4049/jimmunol.1500283.

Ctr2 regulates mast cell maturation by affecting the storage and expression of tryptase and proteoglycans

Helena Öhrvik[*,§], **Brandon Logeman**[†], **Glyn Noguchi**[†], **Inger Eriksson**[*], **Lena Kjellén**[*], **Dennis J. Thiele**[†], and **Gunnar Pejler**[*,‡,§]

[*]Uppsala University, Department of Medical Biochemistry and Microbiology, Uppsala, 751 23 Sweden

[†]Duke University School of Medicine, Department of Pharmacology and Cancer Biology, and Department of Biochemistry, Durham, North Carolina 27710 USA

[‡]Swedish University of Agricultural Sciences, Department of Anatomy, Physiology and Biochemistry, Uppsala, 75651 Sweden

Abstract

Copper (Cu) is essential for multiple cellular functions. Cellular uptake of Cu^{+} is carried out by the Ctr1 high affinity Cu transporter. The mobilization of endosomal Cu pools is regulated by a protein structurally similar to Ctr1, called Ctr2. It was recently shown that ablation of Ctr2 caused an increase in the concentration of Cu localized to endolysosomes. However, the biological significance of excess endolysosomal Cu accumulation has not been assessed. Here we addressed this issue by investigating the impact of Ctr2 deficiency on mast cells, a cell type unusually rich in endolysosomal organelles (secretory granules). We show that $Ctr2^{-/-}$ mast cells have increased intracellular Cu concentrations and that the absence of Ctr2 results in increased metachromatic staining, the latter indicating an impact of Ctr2 on the storage of proteoglycans in the secretory granules. In agreement with this, the absence of Ctr2 caused a skewed ratio between proteoglycans of heparin and chondroitin sulfate type, with increased amounts of heparin accompanied by a reduction of chondroitin sulfate. Moreover, transmission electron microscopy analysis revealed a higher number of electron dense granules in $Ctr2^{-/-}$ mast cells than in wild-type cells. The increase in granular staining and heparin content is compatible with an impact of Ctr2 on mast cell maturation and, in support of this, the absence of Ctr2 resulted in markedly increased mRNA expression, storage and enzymatic activity of tryptase. Taken together, the present study introduces Ctr2 and Cu as novel actors in the regulation of mast cell maturation and granule homeostasis.

Introduction

The essential metal copper (Cu) has many fundamental functions in maintenance of normal growth and development (1–4). Due to its redox activity, Cu is a crucial component in

[§]Corresponding author's contact information: Uppsala University, Department of Medical Biochemistry and Microbiology, Biomedical Center, Husargatan 3, 75123 Sweden, Phone: +48-18-4714442, Fax: +46-18-4714382, gunnar.pejler@imbim.uu.se; helena.ohrvik@imbim.uu.se.

enzymes involved in basic cellular functions including cellular respiration and protection towards oxidative stress. The two proteins Ctr1 and Ctr2 are critical to acquire and sustain cellular Cu homeostasis (5–8). Ctr1 transports Cu across the cell membrane into the cell and its importance is reflected by previous studies showing that the genetic ablation of Ctr1 causes embryonic lethality (9, 10). To elucidate the biological function of Ctr2, which mainly localizes to intracellular vesicles, the corresponding gene was genetically targeted in a recent study (7). Although the absence of Ctr2 in mice did not affect their viability or fertility, it was found that $Ctr2^{-/-}$ mice showed an increased concentration of Cu in several organs, in punctate foci in mouse brain, and further studies on $Ctr2^{-/-}$ embryonic fibroblasts suggested that the excess Cu was mainly located in endolysosomal compartments (7).

Mast cells (MCs) are hematopoietic cells of the immune system. They are well known to have a major detrimental impact on various inflammatory conditions such as allergic reactions, but are also known to negatively influence an array of additional pathological conditions (11–13). A hallmark feature of MCs is their high content of highly electron dense secretory lysosomes (granules), which are filled with large quantities of inflammatory mediators such as biogenic amines (histamine, serotonin), cytokines, serglycin proteoglycans, and various proteases, the latter including chymases, tryptases and carboxypeptidase A3 (CPA3) (11, 14). When MCs are activated, e.g. by IgE receptor crosslinking, the contents of these granules are released to the exterior, a process that can lead to a powerful inflammatory reaction (15).

Previous studies have shown that MC granule composition is critically dependent on a dynamic electrostatic interaction between the various granule compounds. Most strikingly, the absence of highly negatively charged proteoglycans of serglycin type causes a dramatic reduction in the storage of various positively charged compounds such as chymase, tryptase, CPA3 and various biogenic amines (16–20). Conversely, the absence of multiple positively charged proteases causes a decrease in the storage of proteoglycans (21). Moreover, previous studies have shown that the absence of histamine results in reduced storage of both proteoglycans and proteases (22), and that the various amines of the granules are mutually interdependent on each other for adequate storage (23, 24). Together, these studies suggest that the composition of the MC granules is regulated through a dynamic balance between compounds of opposite electrical charge.

Although a recent study on Ctr2-deficiency revealed an aberrant accumulation of copper in endolysosomal compartments of mouse embryonic fibroblasts (7), the biological significance of excess Cu accumulation in these types of organelles has not been addressed. Moreover, it is not known whether the biological impact of Ctr2 on Cu homeostasis may be different among individual cell lineages. Here we reasoned that MCs, since they have a remarkably high content of organelles with endolysosomal origin (secretory granules), might be particularly sensitive to aberrant Cu accumulation. To address this, we studied the impact of Ctr2-deficiency on the development and function of MCs. In agreement with our hypothesis, we report that the absence of Ctr2 has major effects on the homeostasis of MC granules.

Materials and Methods

Animals

$Ctr2^{-/-}$ mice were described previously (7). Mice were all on C57BL/6J genetic background and housed at the Duke University Laboratory animal facility, Durham, North Carolina, USA. All procedures for animals were approved by the Institutional Animal Care and Use Committee at Duke University.

Peritoneal lavage

Peritoneal lavage was preformed in 4 weeks old $Ctr2^{+/+}$ and $Ctr2^{-/-}$ animals using 5ml PBS/animal. Cells were kept at 4°C until used for cytospins and protease activity measurements (as described bellow).

BMMC isolation and culture

Bone marrow derived MCs (BMMCs) from $Ctr2^{+/+}$ and $Ctr2^{-/-}$ animals were generated as described (25). Mice were euthanized by CO_2, and cleaned bones were immediately placed in cold RPMI supplemented with FBS and stored at 4°C until cells were recovered from the bone marrow. BMMCs were obtained by culturing bone marrow cells in the presence of IL-3, as previously described (25). The cells were grown at 37°C with 5% CO_2 and kept at a concentration of 0.5–1 × 10^6 cells/ml with weekly changes of medium.

Quantitative RT-PCR and immunoblotting

Total RNA from 1 × 10^6 cultured cells was isolated by using NucleoSpin RNA II (Macherey-Nagel), and first-strand cDNA was synthesized using 100 ng RNA as template by iScript cDNA synthesis kit (Bio-Rad) according to the manufacturer's instructions. Gene expression levels were determined by quantitative RT-PCR (qPCR) using the primer pairs indicated in Table 1. qPCR was performed using SYBR GreenER SuperMix (Invitrogen), 200 nM primers, and 200 ng cDNA, following the PCR cycling conditions recommended by the manufacturer. Melting curve analysis was performed at the end of every run to ensure product uniformity. The relative amount of cDNA was determined in duplicate and calculated according to the $2^{-\Delta\Delta CT}$ method. Glyceraldehyde 3-phosphate dehydrogenase (GAPDH) was used as housekeeping gene.

SDS-PAGE and immunoblotting were carried out by standard laboratory protocols. Total proteins from of 0.2 – 0.5 × 10^6 cells were solubilized in SDS-PAGE sample buffer containing 5% DTT and loaded onto 4–20% gradient gels. Primary antibodies used were against mouse MC protease 6 (mMCP6) (1:1000), CPA3 (1:500), mMCP4 (1:500), mMCP5 (1:500) (raised in rabbit as previously described (25), Histone 3 (1:2500), Histone 2B (1:2500) (Abcam). Anti-actin (1:2000; Santa Cruz) was used as loading control and was probed on the same membrane after stripping. Horseradish peroxidase-conjugated anti-goat or anti-rabbit IgG (GE Healthcare Bio-Sciences) was used as secondary antibody for detection of chemiluminescence with ChemiDoc (Bio-Rad); fluorescence-labeled anti-rabbit and anti-goat IgG was used for detection of fluorescence using an Odyssey Infrared Imager (Li-Cor).

Cell metal measurements

Intracellular Cu, Mn, and Zn concentrations were measured by Inductively Coupled Plasma – Mass Spectrometry (ICP-MS) (NexION 300D, Perkin Elmer) after digestion of cell pellets in HNO_3 (TraceSelect, Fluka). The instrument was stabilized for at least 45 min before optimization of the system using the SmartTune™ function in the control software. The MS-method used 3 replicate readings of 30 sweeps over the analyte mass-range with an integration time of 75 ms for each mass per sweep. The sample aspiration rate was 0.3 mL/min and a sample pre-flush of 60 s was used. The average signals were used to evaluate the elemental concentrations.

Staining of BMMCs, Peritoneal cells and tissue MCs

BMMCs were collected onto cytospin slides. Samples were stained with May-Grünwald/Giemsa (Merck) as previously described (25) and subsequently rinsed in water before mounting.

Transmission electron microscopy (TEM) was performed as previously described (16). Coded counting of cells containing electron dense granules was performed by four independent individuals for at least 100 cells over 10 fields of vision per genotype.

For tryptase staining, cytospin slides were incubated for 30 min with a solution of 10 mM Z-Gly-Pro-Arg 4-methoxy-2-naphtylamine (Sigma) in 0.5 M Tris-HCl (pH 7.5) and 5 mg/ml Fast Garnet GBC sulfate salt (Sigma). Coded counting of intensively stained cells was performed for at least 200 cells over 10 fields of vision per genotype.

Ear skin tissue was fixed in 4% paraformaldehyde/PBS, embedded in paraffin, sectioned, deparafinized and stained with toluidine blue solution (0.1% toluidine blue in 0.17 mM NaCl [pH 2]).

Ear skin sections were deparafinized and stained using the chloroacetate esterase procedure as previously described (25) and subsequently rinsed in water before mounting.

Ear skin sections were deparafinized and microwaved 10 min for antigen retrieval. Vectastain ABC kit (Vector Lab) was used according to the instructions of the manufacturer. Primary antibody anti-mMCP6, (1:100) were diluted in 5% normal goat serum in PBS and incubated over night at 4°C. Slides were incubated with HRP polymer and the signal was visualized using freshly prepared DAB plus chromogen and substrate mix. After the final step, the slides were washed in distilled H_2O, counterstained with hematoxylin and mounted. Pictures were taken using a Leica brightfield microscope.

Degranulation measurement

Cells were sensitized with IgE anti-trinitrophenyl (TNP) at 1 μg/ml or IgE anti-dinitrophenyl (DNP) at 0.1 μg/ml overnight at 37°C. After washing, cells were resuspended in Tyrode's buffer (25) and stimulated with TNP-OVA (0.4 μg/ml) or DNP-HSA (0.01–0.5 μg/ml) for 1 h. Alternatively, incubation with 1 μM calcium ionophore A23187 for 1 h was used to induce MC degranulation. Media and cell fractions were frozen and stored at −20°C until analysis. β-Hexosaminidase activity was assayed as described (25).

Proteoglycan analysis

Heparin and chondroitin sulfate analysis by RPIP-HPLC was performed with 5×10^6 cells as described previously (26).

Protease activity

Protease activity measurements were mainly carried out with standard protocols as described previously (25, 27). The chromogenic substrates S-2288 and S-2586 (for detection of trypsin-like activity/tryptase and chymase-like activity/chymase) were from Chromogenix (Milano, Italy), and M-2245 (for detection of CPA activity) and the fluorogenic substrate I1465 (chymase activity) were from Bachem (Bubendorf, Switzerland). For all measurements, samples were transferred in triplicates into individual wells of 96-well flat-bottom plates, and readings were performed at room temperature using a microplate reader (Infinite; TECAN).

Histamine measurement

Quantification of histamine levels in the BMMCs and supernatants was performed by ELISA according to the manufacturer's instructions (DRG, Germany).

Statistical analysis

All data were derived from at least three independent experiments and are presented as the mean ± S.D. or S.E.M., when appropriate. Each biological replicate corresponds to BMMCs isolated from a single mouse. In total six WT and six $Ctr2^{-/-}$ mice were used to derive the BMMC cultures. Statistical comparisons were performed using a two-tailed *t* test with the assumption of unequal variance. For multiple comparisons, One-Way ANOVA with a Bonferroni correction was performed.

Results

Ctr2 knockout BMMCs accumulate excess Cu

First we evaluated the steady state levels of expression of Ctr1 and Ctr2 mRNA in MCs by qRT-PCR analysis. For this purpose, we used bone marrow derived MCs (BMMCs). As expected, $Ctr2^{-/-}$ BMMCs lacked Ctr2 mRNA. Further, it was noted that the expression of Ctr1 was similar in wild-type (WT) and $Ctr2^{-/-}$ MCs, indicating that the genetic ablation of Ctr2 does not lead to a compensatory effect on the expression of Ctr1 (Fig. 1A). To evaluate the role of Ctr2 in MCs, we next analyzed the Cu concentration in MCs derived from either WT or $Ctr2^{-/-}$ mice. As seen in Fig. 1B, there was a significant elevation of steady state Cu levels in $Ctr2^{-/-}$ cells as compared to WT cells. In contrast, no significant differences in the accumulation of manganese (Fig. 1C) or zinc (data not shown) were observed between WT and $Ctr2^{-/-}$ BMMCs (Fig. 1B). Hence, these data are in agreement with the previous study showing an increase in Cu in mouse cells and tissues lacking Ctr2 (7) and indicate that the effect of the Ctr2 knockout is Cu-specific as opposed to effecting other metals tested.

Ctr2$^{-/-}$ BMMCs show an increased degree of maturation

The data above suggest that Ctr2$^{-/-}$ MCs accumulate high levels of intracellular Cu and, based on previous studies (7), it is likely that this excess Cu is localized to endolysosomal compartments. In MCs, secretory granules constitute the dominating endolysosome-like organelles, and we therefore hypothesized that an excess accumulation of Cu in such compartments might affect their homeostasis. Highly negatively charged proteoglycans of serglycin type are major constituents of MC granules, and it has been demonstrated that serglycin is essential for biogenesis of the MC granules by promoting the storage of other granule compounds (16–19). Conceivably, excess accumulation of Cu could affect granule proteoglycans by, e.g., providing extra positive charge that might electrostatically interact with proteoglycans and thereby impact on their storage. To evaluate this hypothesis we first stained BMMCs with May-Grünwald/Giemsa, a dye that produces the typical metachromatic staining of MC granules. Importantly, metachromatic staining of MC granules with May-Grünwald/Giemsa is strictly dependent on the presence of serglycin proteoglycan, as shown by abrogated staining in serglycin-deficient MCs (16, 17). As shown in Fig. 2A, BMMCs from both WT and Ctr2$^{-/-}$ mice stained positively with May-Grünwald/Giemsa. However, cells lacking Ctr2 showed a markedly more intense staining than did WT cells, and had reduced numbers of immature granules (arrows) compared to the WT cells (Fig. 2A). In addition, Ctr2$^{-/-}$ cells exhibited a denser and more compact morphology. Altogether, these findings indicate that Ctr2 regulates MC granule homeostasis, at least in part by affecting the levels of stored granule proteoglycans.

To further study the effect of Ctr2-deficiency on MC morphology, we performed transmission electron microscopy (TEM) analysis (Fig. 2B). Approximately equal numbers of granules were found in WT and Ctr2$^{-/-}$ MCs. However, the numbers of highly electron dense granules were markedly increased in Ctr2$^{-/-}$ vs. WT MCs, suggesting a higher extent of maturation (Fig. 2B, C).

A hallmark feature of MCs is their ability to degranulate, and thereby release large amounts of preformed granule constituents (11, 14). Since our data displayed above indicate that Ctr2 has an impact on MC granule homeostasis, we next evaluated whether this affects the functional properties of MCs as reflected by their ability to degranulate. To test this, we activated WT or Ctr2$^{-/-}$ MCs by either IgE receptor crosslinking or by calcium ionophore stimulation, followed by measurement of β-hexosaminidase release. As shown in Fig. 2D, the absence of Ctr2 did not adversely affect the extent of MC degranulation, suggesting that the degranulation signaling pathway is not impaired through the knockout of Ctr2. In fact, when using standard conditions of MC activation, we noted a slight tendency of increased β-hexosaminidase release in Ctr2$^{-/-}$ as opposed to WT cells. In order evaluate this in further detail, we performed a dose response experiment with increasing concentrations of IgE receptor-crosslinking antigen. The results from this experiment showed a tendency towards an increase in β-hexosaminidase release in Ctr2$^{-/-}$ vs. WT MCs at low doses of antigen (Fig 2E). However, this increase in sensitivity to antigen-induced degranulation between Ctr2$^{-/-}$ and WT MCs was not statistically significant.

Ctr2$^{-/-}$ BMMCs contain more heparin and less chondroitin sulfate proteoglycans than WT cells

To provide further insight into the impact of Ctr2 on MC proteoglycans, we performed a detailed analysis of the proteoglycan content of WT vs. Ctr2$^{-/-}$ BMMCs. To this end we used an approach where the glycosaminoglycan (GAG) side chains of the proteoglycans were depolymerized to disaccharide units by enzymatic digestion, followed by HPLC separation to determine the structure of the respective disaccharides (26). This structural analysis revealed that chondroitin sulfate (composed of repeating disaccharide units of the general structure: hexuronic acid (HexA)-N-acetylgalactosamine (GalNAc)) was the main type of GAG produced by both WT and Ctr2$^{-/-}$ BMMCs. In addition, both WT and Ctr2$^{-/-}$ BMMCs contained GAGs of heparin type (composed of repeating disaccharide units of the general structure: HexA-N-acetylglucosamine (GlcNAc)). Interestingly, the absence of Ctr2 resulted in a decrease in the total amount of chondroitin sulfate recovered from the BMMCs (Fig. 3A). At the structural level, this was explained by reduced amounts of, in particular, 4-O-sulfated disaccharides of the structure HexA-GalNAc(4-O-SO_3) (denoted 4S), and of the disulfated HexA-GalNAc(4,6-di-O-SO_3) (4S6S) species (Fig. 3A, C). It was also noted that the reduction of chondroitin sulfate in Ctr2$^{-/-}$ cells was accompanied by a profound increase of the heparin content (Fig. 3B). The total increase in heparin was mostly due to a marked (~2-fold) increase in the levels of disulfated disaccharides of HexA-GlcNSO_3(6-O-SO_3) (NS6S) structure and in an even more profound (~4-fold) increase of the tri-sulfated HexA(2-O-SO_3)-GlcNSO_3(6-O-SO_3) (NS6S2S) disaccharide species (Fig. 3B, D).

In order to provide insight into the mechanism underlying the effect of Ctr2 loss on the proteoglycan content of MCs we evaluated whether the absence of Ctr2 could affect the expression of the various enzymes that account for proteoglycan biosynthesis. Fig. 3E depicts some of the important enzymatic steps in the biosynthesis of heparin (and heparan sulfate) and chondroitin sulfate, and indicates the enzymes responsible for the respective biosynthetic steps. To investigate the impact of Ctr2 on the expression of the corresponding genes, we quantified the mRNA levels for the genes corresponding to the enzymes depicted bold. As shown in Fig. 3F, the absence of Ctr2 did not affect the expression of *Xyl1*, *Xyl2*, *C4st*, *Ndst2*, *Ext1*, *Ext2*, *Hs2st* or *Hs6st2*. However, we noted a moderate but statistically significant increase in the expression of *Hs6st1*, coding for one of the sulfotransferase isoforms that introduces 6-O-sulfation of GAGs of heparin type (28). The latter finding is thus in clear agreement with the increase in the levels of 6-O-sulfated heparin disaccharides seen in MCs lacking Ctr2.

Ctr2 knockout BMMCs have increased chymase and tryptase activity

Previous studies have shown that proteoglycans have a crucial role in regulating the composition of MC secretory granules. Most strikingly, the main proteoglycan species expressed by MCs, i.e. serglycin, has been shown to be essential for proper storage of a number of MC-restricted proteases (16, 17). Since our findings suggest a role for Ctr2 in regulating the amounts of proteoglycans in MCs, we next considered the possibility that this could have an impact on the storage of MC granule proteases. To address this we assessed the content of tryptase, one of the major granule proteases, in WT and Ctr2$^{-/-}$ BMMCs. For this purpose we first evaluated cytospin slides of BMMCs by fast garnet staining, a method

that will detect trypsin-like enzymatic activity. As seen in Fig. 4A, Ctr2$^{-/-}$ MCs stained more intensely than WT cells, suggesting higher levels of trypsin-like proteolytic activity (quantification of data is shown in Fig. 4B). Since numerous proteases are known to have trypsin-like enzymatic activity it was important to establish whether this was due to MC tryptase or to any other trypsin-like enzymes that may be expressed by MCs. Since mouse MC protease 6 (mMCP6) is the major form of tryptase expressed by BMMCs we hypothesized that this tryptase accounted for the detected activity. Indeed, when BMMCs derived from mMCP6$^{-/-}$ mice were evaluated, the fast garnet staining was completely abolished (Fig. 4A). In further agreement with an impact of Ctr2 on tryptase storage, experiments using a chromogenic substrate for trypsin-like enzymes revealed increased trypsin-like activity in Ctr2$^{-/-}$ BMMCs vs. WT controls (Fig. 4C). To investigate whether the absence of Ctr2 affects other proteases present in MC granules, we also measured the levels of CPA- and chymotrypsin-like activity in the MCs. Similar to the effects on trypsin-like activity, we noted an increase of chymotrypsin-like activity in Ctr2$^{-/-}$ vs. WT BMMCs whereas, in contrast, the absence of Ctr2 did not affect the levels of CPA activity (Fig. 4C).

Next, we investigated whether the altered levels of enzymatic activities were reflected at the protein levels, by assessing the levels of individual MC proteases by immunoblot analysis. In agreement with the effects of Ctr2 absence on enzymatic activities, we noted a robust increase in mMCP6 protein in cells lacking Ctr2, and there was also an increase in the levels of the chymase mMCP4, the latter being the major chymase expressed by connective tissue type MCs (29). In contrast, the levels of CPA3 and mMCP5 were not affected by the absence of Ctr2. Conceivably, the effects of Ctr2 deficiency on the levels of the respective MC proteases could be a result of altered storage, but there is also the possibility that the altered protease levels could be explained by effects at the mRNA level. To evaluate the latter possibility we assessed the levels of mRNA coding for the different enzymatically active MC proteases by qRT-PCR analysis. This analysis revealed a clear and significant increase in the expression of the mMCP6 gene (*Mcpt6*) in Ctr2$^{-/-}$ vs. WT BMMCs (Fig. 4E), suggesting that the increased levels of mMCP6 protein in Ctr2$^{-/-}$ cells, at least partly, can be explained by increased *Mcpt6* expression. The gene expression of mMCP4 (*Mcpt4*) was affected in a similar fashion as was Mcpt6, being slightly increased in the Ctr2$^{-/-}$ vs. WT BMMCs (Fig. 4E). In contrast, the absence of Ctr2 did not affect the expression of the genes coding for mMCP1 (*Mcpt1*), mMCP5 (*Mcpt5/Cma1*) or CPA3 (*Cpa3*) (Fig. 4E). The chymase, mMCP1, is predominantly expressed in mucosal mast cells (30). Hence, at the mRNA level, the Ctr2$^{-/-}$ cells do not show any alterations towards mucosal MC phenotype compared to the WT BMMCs.

It has been reported that the expression of several MC protease genes, including *Mcpt6* and *Mcpt4*, is regulated by the expression of microphthalmia-associated transcription factor (Mitf) (31, 32). To search for the mechanism behind the upregulated expression of *Mcpt6* we reasoned that this might be explained by effects at the level of Mitf, and tested this hypothesis by assessing the levels of Mitf mRNA in WT and Ctr2$^{-/-}$ BMMCs. Indeed, the expression of Mitf was significantly higher in Ctr2$^{-/-}$ BMMCs vs. WT controls (Fig. 4F), and it is therefore plausible that the elevated *Mcpt6* and *Mcpt4* expression in Ctr2$^{-/-}$ cells is due to upregulation of Mitf. In addition, we analyzed the gene expressions of the

transcription factors Gata1, Gata2, and PU.1 that all are known be important for the differentiation of the common myeloid progenitor into mast cells (33). However, no differences in gene expression of these transcription factors were detected in Ctr2$^{-/-}$ BMMCs vs. WT controls (Fig. 4F).

A recent study showed that tryptase, in addition to having pro-inflammatory effects after its release upon MC degranulation, can have an impact on the intracellular processing of core histones into N-terminally truncated forms (34). In particular, histone 3 (H3) and H2B were sensitive to tryptase-catalyzed truncation. Since our data revealed a marked upregulation of tryptase levels in Ctr2$^{-/-}$ MCs, we hence hypothesized that this could result in effects on core histone processing. Indeed, we found that there was a marked increase in the processing of both H3 and H2B in cells lacking Ctr2 (Fig. 4G), and it is thus likely that this was a result of increased tryptase expression.

Ctr2$^{-/-}$ BMMCs show decreased histamine levels

In addition to promoting the storage of MC-restricted proteases, it has been shown that proteoglycans are important for the storage of histamine in MC granules (18, 19). Since our data indicate that proteoglycan levels are altered in Ctr2$^{-/-}$ MCs, we reasoned that this could also affect the levels of histamine. We investigated this possibility by measuring steady state levels of histamine in WT vs. Ctr2$^{-/-}$ MCs by ELISA. As shown in Fig. 5A, histamine levels were markedly reduced in the Ctr2$^{-/-}$ MCs as compared to WT cells (Fig. 5A), a conceivable explanation being that the decrease of chondroitin sulfate in favor of heparin seen in Ctr2$^{-/-}$ MCs adversely affects the storage of histamine. Another plausible explanation for this could be that the absence of Ctr2 adversely affects the expression of histidine decarboxylase (encoded by *Hdc*), i.e. the enzyme that converts histidine to histamine. However, the steady state levels of *Hdc* expression were significantly higher in Ctr2$^{-/-}$ vs. WT MCs (Fig 5B), arguing against this possibility. To evaluate whether the absence of Ctr2 affects the release of histamine, we stimulated WT and Ctr2$^{-/-}$ MCs with either calcium ionophore or by IgE receptor cross-linking, followed by quantification of released histamine. As depicted in Fig. 5C, there was a significant increase of histamine release from the Ctr2$^{-/-}$ BMMCs after IgE stimulation in comparison with WT cells, and there was a similar tendency after treatment with calcium ionophore. Hence, these data support the notion that Ctr2$^{-/-}$ MCs are slightly more eager to degranulate in response to stimulation than are corresponding WT cells.

MCs from Ctr2$^{-/-}$ mice display augmented chymase and tryptase expression *in vivo*

To investigate whether the effects of Ctr2 deficiency on cultured MCs are manifested *in vivo*, we first investigated if peritoneal MCs were affected by the absence of Ctr2. Toluidine blue staining of the peritoneal cells did not reveal any obvious differences in morphology between WT and Ctr2$^{-/-}$ MCs (data not shown). However, as shown in Fig. 6A, Ctr2$^{-/-}$ peritoneal MCs contained higher levels of tryptase activity compared to WT MCs, when quantifying tryptase-like activity with a chromogenic substrate (Fig. 6A). In line with this we noted a stronger staining for tryptase-like activity when using the fast garnet staining procedure (Fig. 6B). Moreover, the level of chymotrypsin-like (chymase) activity was

higher in peritoneal cell populations from Ctr2$^{-/-}$ mice as compared with WT controls (Fig. 6C).

To extend these *in vivo* findings to another compartment, we also assessed mature MCs in the ear skin. Similar to the peritoneal MC population, WT and Ctr2$^{-/-}$ ear skin MCs stained with approximately equal intensity using toluidine blue (Fig. 6D). In further agreement with the data on the peritoneal MCs, Ctr2$^{-/-}$ ear skin MCs contained higher levels of chymase activity compared to WT MCs, as determined by the chloroacetate esterase procedure (Fig. 6E). Moreover, Ctr2$^{-/-}$ ear skin MCs contained higher levels of mMCP6 compared to WT MCs as determined by immunohistochemical analysis (Fig. 6F, G). These data suggest that loss of Ctr2 not only increases chymase and tryptase levels in BMMCs but also that mature MCs in Ctr2$^{-/-}$ animals have increased chymase and tryptase expression. Moreover, these observations support the hypothesis that loss of Ctr2 and intracellular accumulation of Cu will affect the expression and activity of chymase and tryptase in MCs.

Discussion

The acquisition of Cu is critical for normal growth and development and changes in Cu homeostasis are associated with human immune system alterations, metabolic disease, cancer, neurodegeneration and other disorders (35–38). While the anti-microbial role of Cu in neutrophils and in macrophages are becoming recognized and partly understood (39–41), the potential role of Cu and Cu transporters in MCs have so far not been thoroughly explored. Here we addressed this issue, and show that the absence of Ctr2 has a major impact on the homeostasis of MC secretory granules, as well as on functional properties of MCs. Hence, the present study introduces Ctr2 as a novel regulator of MC functionality, playing a hitherto unrecognized role in the regulation of MC secretory granule homeostasis.

We show that the absence of Ctr2 results in profound effects on the MC proteoglycans (of serglycin type), a primary finding being that the absence of Ctr2 led to an increase in heparin vs. chondroitin sulfate proteoglycan. It is well established that the proteoglycan content differs substantially among MCs of different subclasses, with connective tissue type MCs mainly expressing serglycin proteoglycans with heparin side chains, whereas mucosal type MCs predominantly express chondroitin sulfate. Under standard culture conditions, the MC population studied here, i.e. BMMCs, express predominantly proteoglycans of chondroitin sulfate rather than heparin type (42). However, it has been demonstrated that the heparin content of BMMCs can increase as a sign of a higher extent of MC differentiation (43–45). Therefore, our data suggest that Ctr2, and potentially changes in Cu accumulation, can have a role in promoting MC differentiation into a more mature phenotype.

The mechanism behind the impact of Ctr2 on the MC proteoglycans is intriguing. Potentially, one explanation could be that Cu can act as counter-ions that interact with the negatively charged GAG chains of serglycin. The elevated levels of Cu in granules of Ctr2$^{-/-}$ MCs could thus facilitate proteoglycan storage. Notably, heparin has a higher anionic charge density than has chondroitin sulfate, and it is thus conceivable that heparin is more critically dependent on the presence of positively charged counter-ions for adequate storage. This could explain why the absence of Ctr2 favors storage of heparin over

chondroitin sulfate. An alternative explanation could be that Cu affects the biosynthetic machinery operative during proteoglycan synthesis by, e.g., affecting the expression of the respective biosynthetic enzymes. In support of the latter scenario we noted that Ctr2$^{-/-}$ MCs exhibited an increase in the expression of *Hs6st1*, i.e. the gene coding for one of the sulfotransferases responsible for incorporation of 6-O-sulfate into heparin. Notably, this is in good agreement with our observed increase in the levels of various 6-O-sulfated heparin disaccharides in Ctr2$^{-/-}$ cells. We cannot at present with certainty distinguish between the relative contribution of these alternative mechanisms to the observed effects on proteoglycan levels. In fact, a plausible scenario could be that the observed effects on proteoglycan levels may represent a combined effect of these mechanisms.

A major finding of this investigation was that the absence of Ctr2 led to a profound increase in the levels of mMCP6, mMCP6 being the major tryptase found in BMMCs and the tryptase that most likely is the murine homologue to human β-tryptase (30). Previous studies have shown that the storage of tryptase in MCs is highly dependent on heparin proteoglycan, as shown by the dramatic decrease in mMCP6 storage in MCs lacking *Ndst2* (18, 19). Hence, a likely explanation for the increase in mMCP6 levels in Ctr2$^{-/-}$ cells could be that the increase in heparin may facilitate mMCP6 storage. In agreement with such a scenario, a previous study has shown that mMCP6 storage is severely defective in MCs lacking the expression of heparin 6-O-sulfotransferases (46). In further agreement, it is striking to note that the absence of Ctr2 led to increased expression of *Hs6st1* accompanied by increased 6-O-sulfation of heparin. However, adding complexity to this issue, our data indicate that the absence of Ctr2 leads to increased expression of the mMCP6 gene (*Mcpt6*), suggesting that effects on gene expression could contribute to the increase in tryptase levels. We also found that there was an upregulated gene expression of Mitf in Ctr2$^{-/-}$ MCs. Since *Mcpt6* expression has been shown to depend strongly on this transcription factor (32), it is thus likely that the upregulated *Mcpt6* expression is directly linked to the induction of Mitf. Given that also *Mcpt4* (coding for mMCP4) expression has been shown to be directly activated by Mitf (47), it is expected that *Mcpt4* expression is increased in Ctr2$^{-/-}$ cells. However, we only detected a marginal increase in *Mcpt4* expression in cells lacking Ctr2, suggesting that the effects seen on mMCP4 protein levels were due to effects primarily at the level of protein storage.

We cannot at present explain with certainty why the absence of Ctr2 affects the transcription of Mitf. However, studies in melanoma cells suggest that Mitf expression can be influenced by activation of a reactive oxygen species (ROS)-ERK axis (48), and it has recently been shown that Cu homeostasis can affect the activation of ERK (49). Moreover, since Cu is redox active, excessive Cu can increase the cellular formation of reactive oxygen species (50). Consequently, a possible explanation for the *Mcpt6* upregulation could be that Cu affects activation of ERK signaling leading to an alteration in Mitf expression, in turn causing an induction of *Mcpt6*. The relation between gene and protein expression of Mitf and Cu will be the subject of future investigations.

Acknowledgements

We thank members of the Pejler group for suggestions and assistance, A. Boström from the Histopathology at SLU for expert technical assistance, J. Pettersson at Uppsala University for the ICP-MS analysis, and Richard R. Festa for generously performing the peritoneal lavage of the animals.

This work was supported by grants from the Swedish Research Council (524-2014-1 (HÖ) and 521-2013-3870 (GP)) and by grants from The Swedish Cancer Foundation (GP), The Swedish Heart and Lung Foundation (GP), Formas (GP), the Torsten Söderberg Foundation (GP) and NIH grant DK074192 (DJT).

References

1. Kim BE, Nevitt T, Thiele DJ. Mechanisms for copper acquisition, distribution and regulation. Nat Chem Biol. 2008; 4:176–185. [PubMed: 18277979]
2. Nevitt T, Ohrvik H, Thiele DJ. Charting the travels of copper in eukaryotes from yeast to mammals. Biochim Biophys Acta. 2012; 1823:1580–1593. [PubMed: 22387373]
3. Lutsenko S. Human copper homeostasis: a network of interconnected pathways. Curr Opin Chem Biol. 2010; 14:211–217. [PubMed: 20117961]
4. Wang Y, Hodgkinson V, Zhu S, Weisman GA, Petris MJ. Advances in the understanding of mammalian copper transporters. Adv Nutr. 2011; 2:129–137. [PubMed: 22332042]
5. Dancis A, Yuan DS, Haile D, Askwith C, Eide D, Moehle C, Kaplan J, Klausner RD. Molecular characterization of a copper transport protein in S. cerevisiae: an unexpected role for copper in iron transport. Cell. 1994; 76:393–402. [PubMed: 8293472]
6. Lee J, Prohaska JR, Dagenais SL, Glover TW, Thiele DJ. Isolation of a murine copper transporter gene, tissue specific expression and functional complementation of a yeast copper transport mutant. Gene. 2000; 254:87–96. [PubMed: 10974539]
7. Ohrvik H, Nose Y, Wood LK, Kim BE, Gleber SC, Ralle M, Thiele DJ. Ctr2 regulates biogenesis of a cleaved form of mammalian Ctr1 metal transporter lacking the copper- and cisplatin-binding ecto-domain. Proc Natl Acad Sci U S A. 2013; 110:E4279–E4288. [PubMed: 24167251]
8. Zhou B, Gitschier J. hCTR1: a human gene for copper uptake identified by complementation in yeast. Proc Natl Acad Sci U S A. 1997; 94:7481–7486. [PubMed: 9207117]
9. Lee J, Prohaska JR, Thiele DJ. Essential role for mammalian copper transporter Ctr1 in copper homeostasis and embryonic development. Proc Natl Acad Sci U S A. 2001; 98:6842–6847. [PubMed: 11391005]
10. Kuo YM, Zhou B, Cosco D, Gitschier J. The copper transporter CTR1 provides an essential function in mammalian embryonic development. Proc Natl Acad Sci U S A. 2001; 98:6836–6841. [PubMed: 11391004]
11. Wernersson S, Pejler G. Mast cell secretory granules: armed for battle. Nat Rev Immunol. 2014; 14:478–494. [PubMed: 24903914]
12. Galli SJ, Grimbaldeston M, Tsai M. Immunomodulatory mast cells: negative, as well as positive, regulators of immunity. Nat Rev Immunol. 2008; 8:478–486. [PubMed: 18483499]
13. Metz M, Maurer M. Mast cells--key effector cells in immune responses. Trends Immunol. 2007; 28:234–241. [PubMed: 17400512]
14. Lundequist A, Pejler G. Biological implications of preformed mast cell mediators. Cell Mol Life Sci. 2011; 68:965–975. [PubMed: 21069421]
15. Blank U, Rivera J. The ins and outs of IgE-dependent mast-cell exocytosis. Trends Immunol. 2004; 25:266–273. [PubMed: 15099567]
16. Braga T, Grujic M, Lukinius A, Hellman L, Abrink M, Pejler G. Serglycin proteoglycan is required for secretory granule integrity in mucosal mast cells. Biochem J. 2007; 403:49–57. [PubMed: 17147513]
17. Abrink M, Grujic M, Pejler G. Serglycin is essential for maturation of mast cell secretory granule. J Biol Chem. 2004; 279:40897–40905. [PubMed: 15231821]

18. Forsberg E, Pejler G, Ringvall M, Lunderius C, Tomasini-Johansson B, Kusche-Gullberg M, Eriksson I, Ledin J, Hellman L, Kjellen L. Abnormal mast cells in mice deficient in a heparin-synthesizing enzyme. Nature. 1999; 400:773–776. [PubMed: 10466727]
19. Humphries DE, Wong GW, Friend DS, Gurish MF, Qiu WT, Huang C, Sharpe AH, Stevens RL. Heparin is essential for the storage of specific granule proteases in mast cells. Nature. 1999; 400:769–772. [PubMed: 10466726]
20. Ringvall M, Ronnberg E, Wernersson S, Duelli A, Henningsson F, Abrink M, Garcia-Faroldi G, Fajardo I, Pejler G. Serotonin and histamine storage in mast cell secretory granules is dependent on serglycin proteoglycan. J Allergy Clin Immunol. 2008; 121:1020–1026. [PubMed: 18234316]
21. Grujic M, Calounova G, Eriksson I, Feyerabend T, Rodewald HR, Tchougounova E, Kjellen L, Pejler G. Distorted secretory granule composition in mast cells with multiple protease deficiency. J Immunol. 2013; 191:3931–3938. [PubMed: 23975861]
22. Ohtsu H, Tanaka S, Terui T, Hori Y, Makabe-Kobayashi Y, Pejler G, Tchougounova E, Hellman L, Gertsenstein M, Hirasawa N, Sakurai E, Buzas E, Kovacs P, Csaba G, Kittel A, Okada M, Hara M, Mar L, Numayama-Tsuruta K, Ishigaki-Suzuki S, Ohuchi K, Ichikawa A, Falus A, Watanabe T, Nagy A. Mice lacking histidine decarboxylase exhibit abnormal mast cells. FEBS Lett. 2001; 502:53–56. [PubMed: 11478947]
23. Garcia-Faroldi G, Rodriguez CE, Urdiales JL, Perez-Pomares JM, Davila JC, Pejler G, Sanchez-Jimenez F, Fajardo I. Polyamines are present in mast cell secretory granules and are important for granule homeostasis. PLoS One. 2010; 5:e15071. [PubMed: 21151498]
24. Csaba G, Kovacs P, Buzas E, Mazan M, Pallinger E. Serotonin content is elevated in the immune cells of histidine decarboxylase gene knock-out (HDCKO) mice. Focus on mast cells. Inflamm Res. 2007; 56:89–92. [PubMed: 17431746]
25. Ronnberg E, Pejler G. Serglycin: the master of the mast cell. Methods Mol Biol. 2012; 836:201–217. [PubMed: 22252637]
26. Dagalv A, Holmborn K, Kjellen L, Abrink M. Lowered expression of heparan sulfate/heparin biosynthesis enzyme N-deacetylase/n-sulfotransferase 1 results in increased sulfation of mast cell heparin. J Biol Chem. 2011; 286:44433–44440. [PubMed: 22049073]
27. Waern I, Lundequist A, Pejler G, Wernersson S. Mast cell chymase modulates IL-33 levels and controls allergic sensitization in dust-mite induced airway inflammation. Mucosal Immunol. 2013; 6:911–920. [PubMed: 23235745]
28. Esko JD, Lindahl U. Molecular diversity of heparan sulfate. J Clin Invest. 2001; 108:169–173. [PubMed: 11457867]
29. Tchougounova E, Pejler G, Abrink M. The chymase, mouse mast cell protease 4, constitutes the major chymotrypsin-like activity in peritoneum and ear tissue. A role for mouse mast cell protease 4 in thrombin regulation and fibronectin turnover. J Exp Med. 2003; 198:423–431. [PubMed: 12900518]
30. Pejler G, Abrink M, Ringvall M, Wernersson S. Mast cell proteases. Adv Immunol. 2007; 95:167–255. [PubMed: 17869614]
31. Kim DK, Morii E, Ogihara H, Lee YM, Jippo T, Adachi S, Maeyama K, Kim HM, Kitamura Y. Different effect of various mutant MITF encoded by mi, Mior, or Miwh allele on phenotype of murine mast cells. Blood. 1999; 93:4179–4186. [PubMed: 10361115]
32. Morii E, Tsujimura T, Jippo T, Hashimoto K, Takebayashi K, Tsujino K, Nomura S, Yamamoto M, Kitamura Y. Regulation of mouse mast cell protease 6 gene expression by transcription factor encoded by the mi locus. Blood. 1996; 88:2488–2494. [PubMed: 8839840]
33. Iwasaki H, Mizuno S, Arinobu Y, Ozawa H, Mori Y, Shigematsu H, Takatsu K, Tenen DG, Akashi K. The order of expression of transcription factors directs hierarchical specification of hematopoietic lineages. Genes & development. 2006; 20:3010–3021. [PubMed: 17079688]
34. Melo FR, Vita F, Berent-Maoz B, Levi-Schaffer F, Zabucchi G, Pejler G. Proteolytic histone modification by mast cell tryptase, a serglycin proteoglycan-dependent secretory granule protease. J Biol Chem. 2014; 289:7682–7690. [PubMed: 24478313]
35. Kaler SG. ATP7A-related copper transport diseases-emerging concepts and future trends. Nat Rev Neurol. 2011; 7:15–29. [PubMed: 21221114]

36. Kim H, Wu X, Lee J. SLC31 (CTR) family of copper transporters in health and disease. Mol Aspects Med. 2013; 34:561–570. [PubMed: 23506889]
37. Prohaska JR, Lukasewycz OA. Effects of copper deficiency on the immune system. Adv Exp Med Biol. 1990; 262:123–143. [PubMed: 2181820]
38. Brady DC, Crowe MS, Turski ML, Hobbs GA, Yao X, Chaikuad A, Knapp S, Xiao K, Campbell SL, Thiele DJ, Counter CM. Copper is required for oncogenic BRAF signalling and tumorigenesis. Nature. 2014; 509:492–496. [PubMed: 24717435]
39. White C, Lee J, Kambe T, Fritsche K, Petris MJ. A role for the ATP7A copper-transporting ATPase in macrophage bactericidal activity. J Biol Chem. 2009; 284:33949–33956. [PubMed: 19808669]
40. Lazarchick J. Update on anemia and neutropenia in copper deficiency. Curr Opin Hematol. 2012; 19:58–60. [PubMed: 22080848]
41. Percival SS. Copper and immunity. Am J Clin Nutr. 1998; 67:1064S–1068S. [PubMed: 9587153]
42. Ronnberg E, Melo FR, Pejler G. Mast cell proteoglycans. J Histochem Cytochem. 2012; 60:950–962. [PubMed: 22899859]
43. Dayton ET, Pharr P, Ogawa M, Serafin WE, Austen KF, Levi-Schaffer F, Stevens RL. 3T3 fibroblasts induce cloned interleukin 3-dependent mouse mast cells to resemble connective tissue mast cells in granular constituency. Proc Natl Acad Sci U S A. 1988; 85:569–572. [PubMed: 3257570]
44. Gurish MF, Ghildyal N, McNeil HP, Austen KF, Gillis S, Stevens RL. Differential expression of secretory granule proteases in mouse mast cells exposed to interleukin 3 and c-kit ligand. J Exp Med. 1992; 175:1003–1012. [PubMed: 1372640]
45. Duelli A, Ronnberg E, Waern I, Ringvall M, Kolset SO, Pejler G. Mast cell differentiation and activation is closely linked to expression of genes coding for the serglycin proteoglycan core protein and a distinct set of chondroitin sulfate and heparin sulfotransferases. J Immunol. 2009; 183:7073–7083. [PubMed: 19915053]
46. Anower EKMF, Habuchi H, Nagai N, Habuchi O, Yokochi T, Kimata K. Heparan sulfate 6-O-sulfotransferase isoform-dependent regulatory effects of heparin on the activities of various proteases in mast cells and the biosynthesis of 6-O-sulfated heparin. J Biol Chem. 2013; 288:3705–3717. [PubMed: 23223449]
47. Jippo T, Lee YM, Katsu Y, Tsujino K, Morii E, Kim DK, Kim HM, Kitamura Y. Deficient transcription of mouse mast cell protease 4 gene in mutant mice of mi/mi genotype. Blood. 1999; 93:1942–1950. [PubMed: 10068667]
48. Kim ES, Park SJ, Goh MJ, Na YJ, Jo DS, Jo YK, Shin JH, Choi ES, Lee HK, Kim JY, Jeon HB, Kim JC, Cho DH. Mitochondrial dynamics regulate melanogenesis through proteasomal degradation of MITF via ROS-ERK activation. Pigment Cell Melanoma Res. 2014; 27:1051–1062. [PubMed: 25065405]
49. Turski ML, Brady DC, Kim HJ, Kim BE, Nose Y, Counter CM, Winge DR, Thiele DJ. A novel role for copper in Ras/mitogen-activated protein kinase signaling. Mol Cell Biol. 2012; 32:1284–1295. [PubMed: 22290441]
50. Pourahmad J, Ross S, O'Brien PJ. Lysosomal involvement in hepatocyte cytotoxicity induced by Cu(2+) but not Cd(2+). Free Radic Biol Med. 2001; 30:89–97. [PubMed: 11134899]

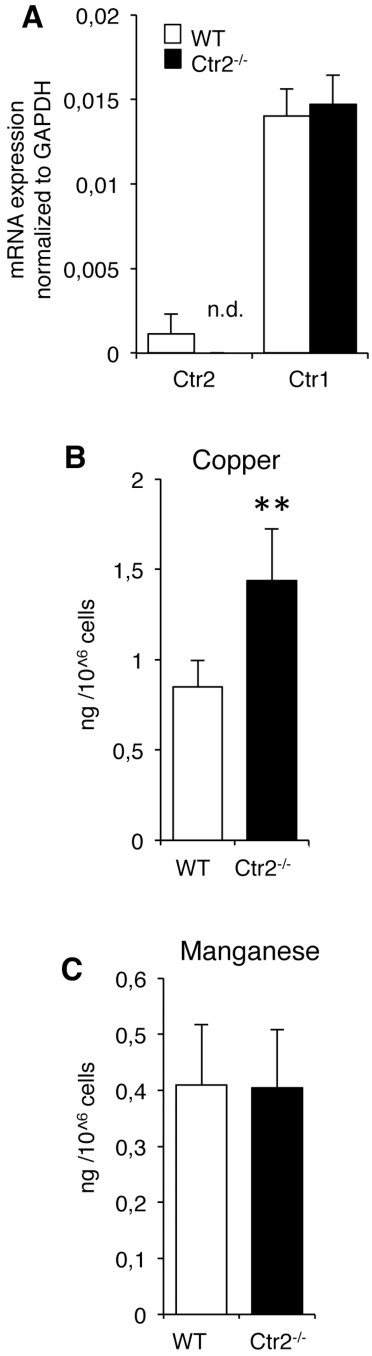

Figure 1.

Loss of Ctr2 results in increased cellular Cu levels. (A) Total RNA was prepared from WT and Ctr2$^{-/-}$ BMMCs and expression of Ctr1 and Ctr2 was analyzed by qPCR (n.d., not detected). Data are presented as mean ± S.E.M. from three biological replicates. (B,C) Total Cu (B) levels and Manganese (C) in WT and Ctr2$^{-/-}$ BMMCs were measured by ICP-MS. Data are presented as mean ± S.D. from five biological replicates. ** $p \leq 0.01$.

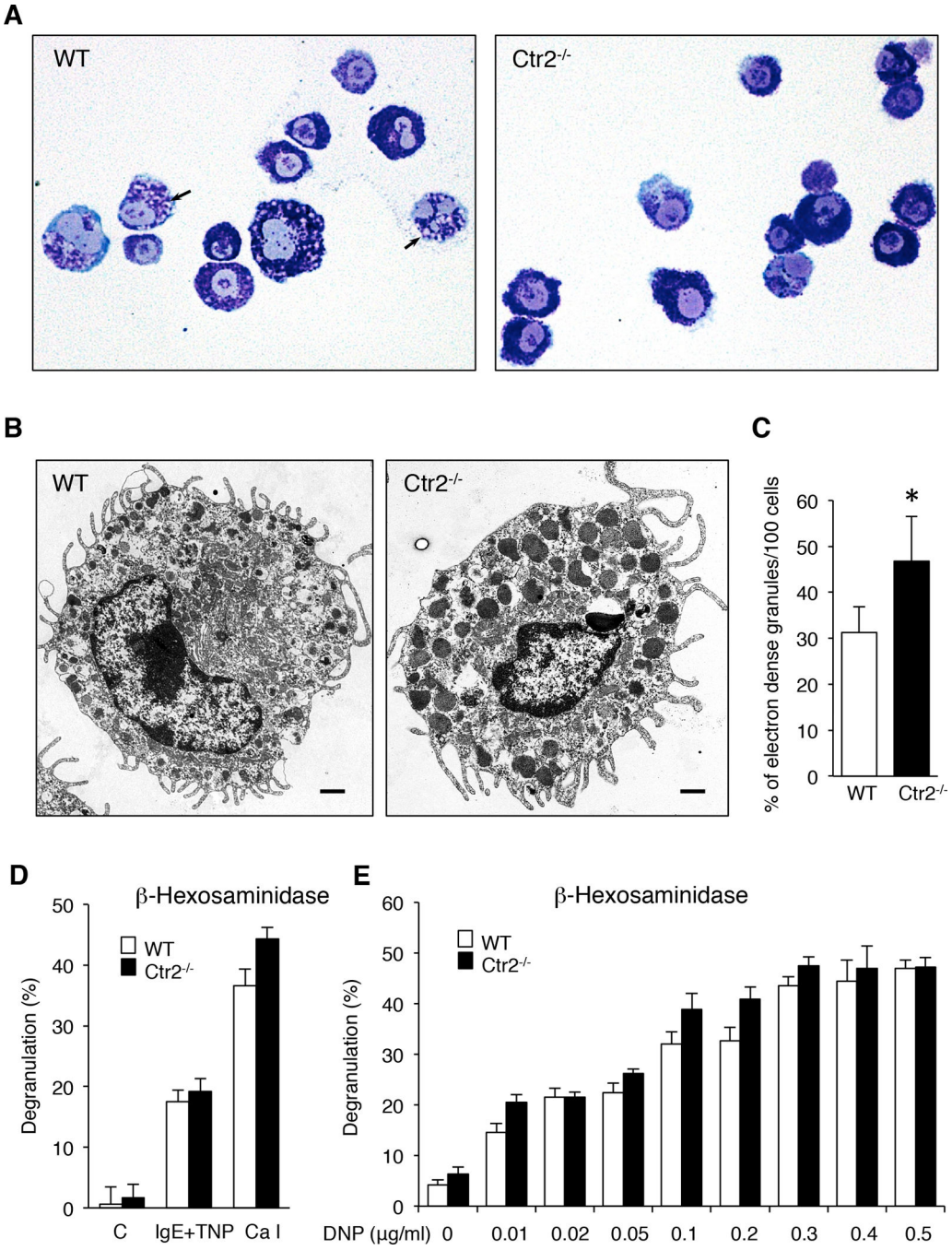

Figure 2.

Ctr2$^{-/-}$ BMMCs show an increased degree of maturation. (A) Cytospin slides were prepared from WT and Ctr2$^{-/-}$ BMMCs and stained with May-Grünwald/Giemsa. Arrows indicate immature granules. Note that immature granules are less frequent in Ctr2−/− BMMCs vs. WT cells. Original magnification × 400. (B) WT and Ctr2$^{-/-}$ BMMCs were subjected to transmission electron microscopy (TEM) analysis. Original magnification × 50000 (Scale bar, 1 μm). Note that granules in Ctr2−/− cells have a higher electron density. (C) Quantification of the number of electron dense granules in WT and Ctr2$^{-/-}$ BMMCs, as

assessed by TEM analysis. (D) Activation of WT and Ctr2$^{-/-}$ BMMCs by IgE crosslinking or calcium ionophore (A23187; Ca I) measured as release of β-hexosaminidase. (E) WT and Ctr2$^{-/-}$ BMMCs were activated by IgE crosslinking at DNP concentrations ranging from 0.01– 0.5 μg/ml. Data are presented as mean ± S.E.M. from four biological replicates, * $p \leq 0.05$.

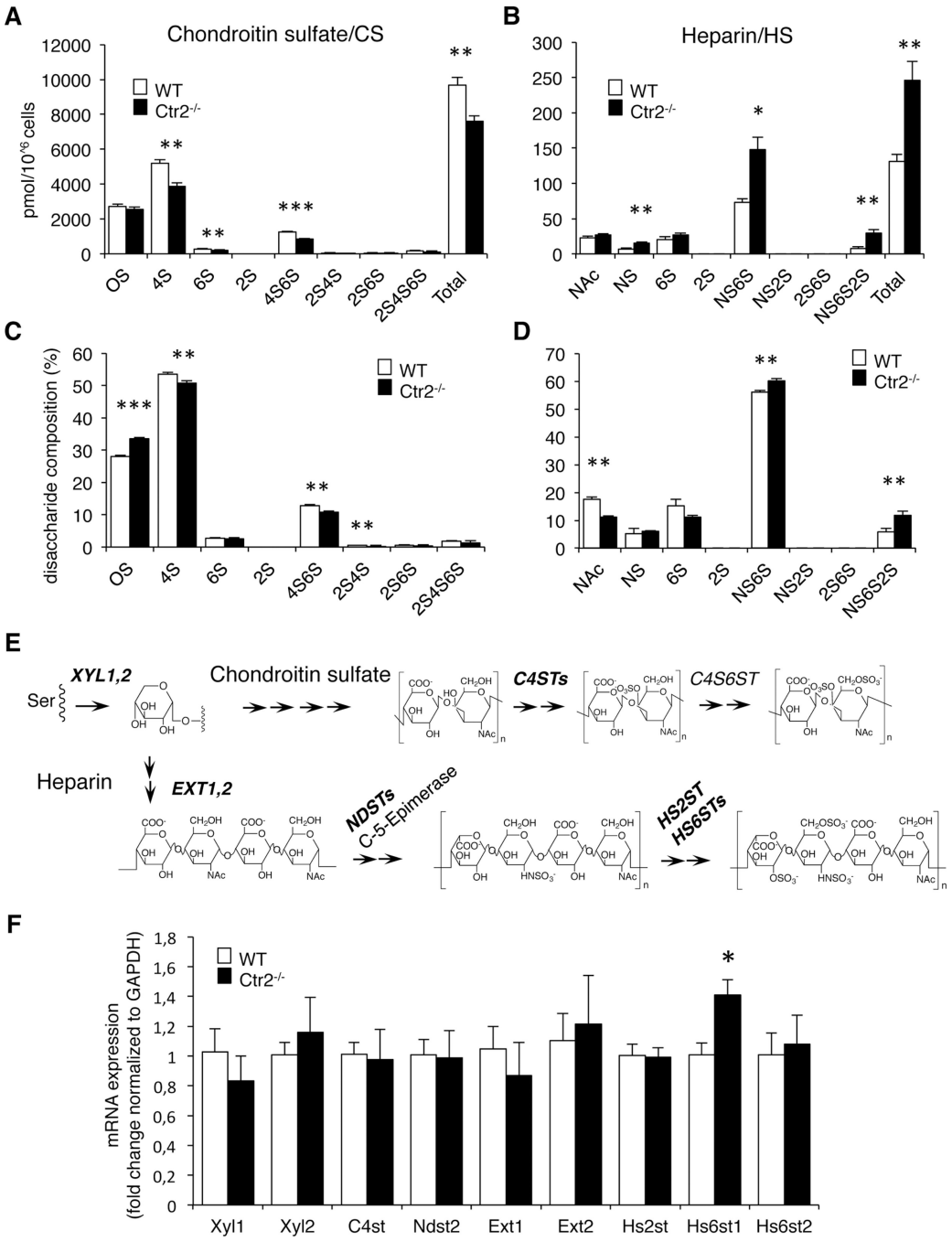

Figure 3.

Ctr2$^{-/-}$ BMMCs contain more heparin and less chondroitin sulfate proteoglycans than WT cells. GAGs were isolated from WT and Ctr2$^{-/-}$ BMMCs, and depolymerized to disaccharides by treatment with chondroitinase ABC and heparinase I, II, and III, respectively. Disaccharides were separated by RPIP-HPLC. (A) The disaccharide composition of chondroitin sulfate (CS) recovered from WT and Ctr2$^{-/-}$ BMMCs. (B) The disaccharide composition of heparin/heparan sulfate recovered from WT and Ctr2$^{-/-}$ BMMCs. (C, D) Percentage of the respective disaccharide units in chondroitin sulfate (C)

and heparin/heparan sulfate (D) recovered from WT and Ctr2−/− cells, respectively. Data are presented as mean ± S.D. from three biological replicates. The disaccharide composition is given as picomoles per 10^6 cells (BMMCs). (E) Schematic figure depicting critical enzymatic steps in heparin and chondroitin sulfate synthesis; analyzed enzymes are indicated in bold. Xyl1/2 catalyze transfer of Xylose residues to Ser residues of the protein core (both in heparin/heparan sulfate and chondroitin sulfate); EXT1/2 catalyze chain elongation in heparin/heparan sulfate; NDSTs catalyze the N-deacetylation and subsequent N-sulfation of selected N-acetylglucosamine (GlcNAc) residues in heparin/heparan sulfate; HS2ST and HS6STs catalyze the 2-O- and 6-O-sufation of heparin/heparan sulfate; C4STs catalyze the 4-O-sulfation of selected N-acetylgalactosamine (GalNAc) residues of chondroitin sulfate. (F) Total RNA was prepared from WT and $Ctr2^{-/-}$ BMMCs and expression of critical enzymes involved in chondroitin sulfate and heparin synthesis were analyzed by qPCR. Data presented as mean ± S.E.M. from three biological replicates. Chondroitin sulfate disaccharides (A, C): OS CS/Hya, nonsulfated disaccharides of chondroitin sulfate or hyaluronan origin; 4S, Hexuronic acid (HexA)-GalNAc(4-*O*-SO_3^-); 6S, HexA-GalNAc(6-*O*-SO_3^-); 2S, HexA(2-*O*-SO_3^-)-GalNAc; 4S6S, HexAGalNAc(4,6-di-*O*-SO_3^-); 2S4S, HexA(2-*O*-SO_3^-)-GalNAc(4-*O*-SO_3^-); 2S6S, HexA(2-*O*-SO_3^-)-GalNAc(6-*O*-SO_3^-); 2S4S6S, HexA(2-*O*-SO_3^-)-GalNAc(4,6-di-*O*-SO_3^-). Heparin/HS disaccharides (B, D): NAc, HexA-GlcNAc; NS, HexA-$GlcNSO_3^-$; 6S, HexA-GlcNAc(6- *O*-SO_3^-); 2S, HexA(2-*O*-SO_3^-)-GlcNAc; NS6S, HexA-$GlcNSO_3^-$(6- *O*-SO_3^-); NS2S, HexA(2-*O*-SO_3^-)-$GlcNSO_3^-$; 2S6S, HexA(2-*O*-SO_3^-)-GlcNAc(6-*O*-SO_3^-); NS6S2S, HexA(2-*O*-SO_3^-)-$GlcNSO_3^-$(6-*O*-SO_3^-). * $p \le 0.05$, ** $p \le 0.01$, *** $p \le 0.001$.

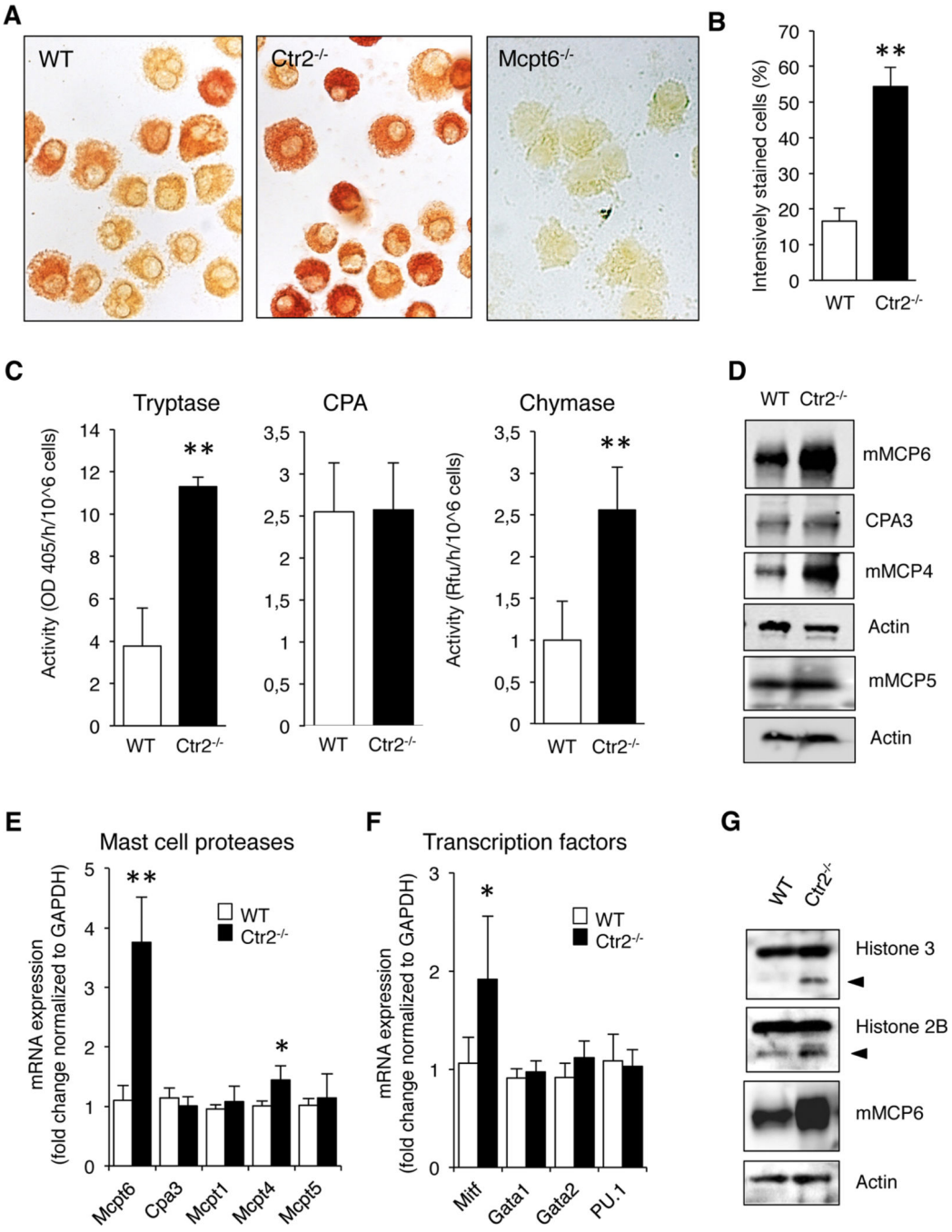

Figure 4.

Ctr2$^{-/-}$ BMMCs exhibit increased chymase and tryptase activity. (A) Cytospin slides were prepared from WT and Ctr2$^{-/-}$ BMMCs and stained for tryptase activity as described in Material and Methods. BMMCs isolated from Mcpt6$^{-/-}$ mice served as negative control for the tryptase activity staining. (B) Quantification of tryptase activity staining in WT and Ctr2$^{-/-}$ BMMCs. (C) Protein extracts isolated from WT and Ctr2$^{-/-}$ BMMCs were assayed for total trypsin-like activity using S-2288, total CPA activity using M-2245, and total chymase-like activity using a fluorescent substrate (Suc-Ala-Ala-Pro-Phe-AMC). Chymase-

like activity is shown as raw fluorescent units (RFU). Total activities are given as activity per hour and 10^6 cells. (D) Protein extracts from WT and Ctr2$^{-/-}$ BMMCs were immunoblotted with anti-mMCP6, anti-CPA3, anti-mMCP4, anti-mMCP5, with anti-actin antibody as loading control. (E) Total mRNA extracts were prepared from WT and Ctr2$^{-/-}$ BMMCs and expression of Mcpt6, Cpa3, Mcpt1, Mcpt4, and Mcpt5 were analyzed with qPCR. (F) Microphthalmia transcription factor (Mitf), GATA1, GATA2, and PU.1 expression was analyzed as in (F). (G) Isolated proteins from WT and Ctr2$^{-/-}$ BMMCs were immunoblotted with anti-histone 3, anti-histone 2B, anti-mMCP6, and anti-actin antibody as loading control. Data are presented as mean ± S.E.M. from three - four biological replicates, * $p \leq 0.05$, ** $p \leq 0.01$, *** $p \leq 0.001$.

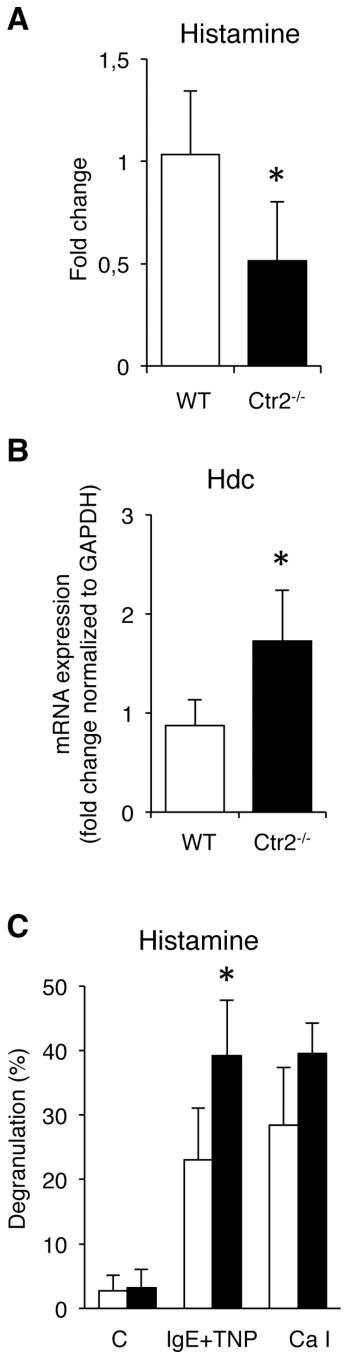

Figure 5.

$Ctr2^{-/-}$ BMMCs have decreased histamine levels. (A) Total cellular histamine levels in WT and $Ctr2^{-/-}$ BMMCs were quantified by ELISA. Data are presented as mean ± S.D. from five biological replicates. (B) Total RNA was prepared from WT and $Ctr2^{-/-}$ BMMCs and expression of histidine decarboxylase (Hdc) was analyzed by qPCR. Data are presented as mean ± S.E.M. from three biological replicates. (C) WT and $Ctr2^{-/-}$ BMMCs were activated by IgE crosslinking or calcium ionophore (A23187; Ca I), followed by measurement of

histamine levels in media and cell pellets. Data are presented as mean ± S.D. from four biological replicates. * $p \leq 0.05$.

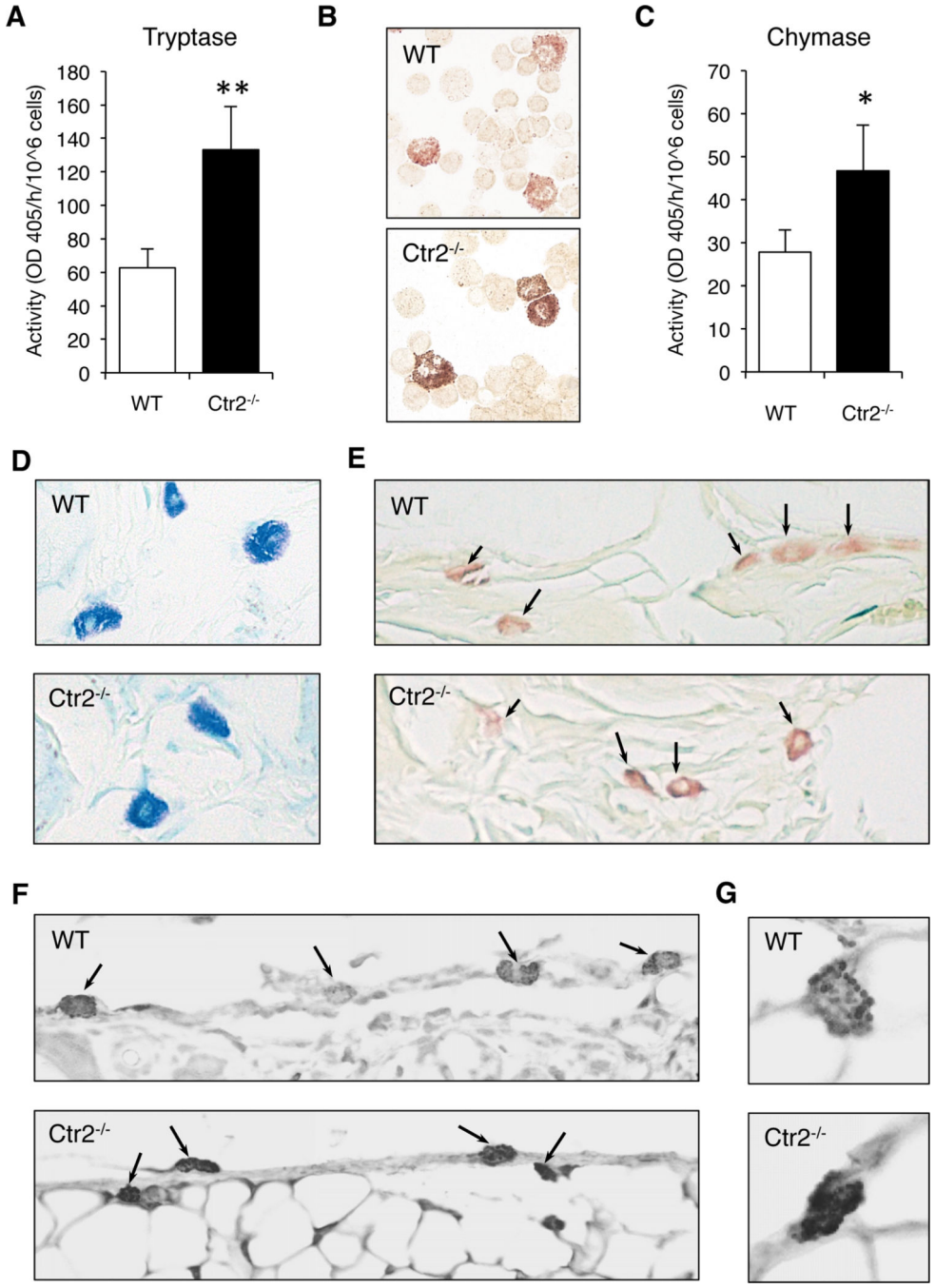

Figure 6.

Mast cells from Ctr2$^{-/-}$ mice display increased chymase and tryptase expression *in vivo*. (A) Protein extracts isolated from WT and Ctr2$^{-/-}$ peritoneal cells were assayed for total trypsin-like activity using the S-2288 chromogenic substrate. (B) Cytospin slides were prepared from WT and Ctr2$^{-/-}$ peritoneal cells and were stained for tryptase activity as described in Materials and Methods. (C) Protein extracts isolated from WT and Ctr2$^{-/-}$ peritoneal cells were assayed for total chymase-like activity using the S-2586 chromogenic substrate. Total activities are given as activity per hour and 10^6 cells. (D–G) Sections were prepared from

ear skin tissue of WT and Ctr2$^{-/-}$ mice. (D) Sections were stained with toluidine blue. (E) Sections were subjected to the chloroacetate esterase assay. (F and G) Sections were subjected to immunohistochemical analysis using anti-mMCP6 antibody. MCs are indicated by arrows. (G) Magnified images of individual MCs. Note the increased of mMCP6 in Ctr2$^{-/-}$ MCs and the granular staining of mMCP6 in both WT and Ctr2$^{-/-}$ MCs. Data are presented as mean ± S.D. from three biological replicates. * $p \leq 0.05$, ** $p \leq 0.01$. Original magnification × 400.

Table 1

Murine primers used for qPCR

Target gene	Forward sequence (5´-3´)	Reverse sequence (5´-3´)
Gapdh	CTC CCA CTC TTC CAC CTT CG	CCA CCA CCC TGT TGC TGT AG
Ctr2	AAC TTC AGA CAA TAG GAC CCG CCT	TAG GAC ATG ACA GCC AGC ATC ACA
Ctr1	GGG CTT ACC CTG TGA AGA CTT TT	AAT GTT GTC GTC CGT GTG GT
Xyl1	GAA CAG CTG CAG GTA CTA CCC AAT	GAA TCG GTC AGC AAG GAA GTA GA
Xyl2	GGG TGA GAC CCG CTT CCT	GCA TCA TCT TTC CTG AGA GGT AGT T
C4st1	CCA AAG TAT GTT GCA CCC AGT	CTG GTC CCG TCT CAT CTG GT
Ndst2	GTG GCT GAT GTT GAG GCT TTG	ATC CTC CTC TTC TGT CCC GG
Ext1	GTG TAC CCG CAG CAG AAA GG	GTA GA ACCT GGA GCC CTC GAT
Ext2	CAA AAT CCG AGT TCC CCT GAA	TCG ATT TCG TCG TAA GGG AAG
Hs2st	CCA TGT CTC CCA GAT CGT GAC	GTT ATA TGT TCT AAG GAC TCA GGC TC
Hs6st1	CAG CCA ACA CGT CTG AAC TG	CTA GAC AAA GAC AAT TAG AAG ACA AC
Hs6st2	AGT GGT ATT CAT GCT TTC AAG AG	CTG CAA ATA TTG TCA CAG AGC TC
Hs6st3	ACT ACA ACA GCC AAG TGG TCA G	TGG ATT GGA AAT GAA GGC AG
Cpa3	TGA CAG GGA GAA GGT ATT CCG	CCA AGG TTG ACT GGA TGG TCT
Mcpt1	GAA GGA ATG GGT CCA GAC AT	ACG GGT CAA CTT CAC ATT CA
Mcpt2	GCCTATCTGAAGTTCACCACTAA	TACAGTGTGCAGCAGTCATC
Mcpt4	GCA GTC TTC ACC CGA AT CTC	CAG GAT GGA CACA TG CTT TG
Mcpt5	CCT GTC TGT AGT TCC TGC TG	CAG TTG ACA ATC TGG GTC TT
Mcpt6	CAT TGA TAA TGA CGA GCC TCT CC	CAT CTC CCG TGT AGA GGC CAG
Mitf	AGA TTT GAG ATG CTC ATC CCC	GAT GCG TGA TGT CAT ACT GGA
Gata1	ATC AGC ACT GGC CTA CTA CAG AG	GAG AGA AGA AAG GAC TGG GAA AG
Gata2	CAA GAA AGG GGC TGA ATG TTT CG	GTG TCC CAC AGG TGC CAT G
Pu.1	AGA GCA TAC CAA CGT CCA ATG C	GTG CGG AGA AAT CCC AGT AGT G
Hdc	GGATTCTGGGTCAAGGACAAGT	AATGCATGAAGTCCGTGGCT